CHIN. PHYS. LETT. Vol. 34, No. 12 (2017) 124202

Visual Passive Ranging Method Based on Re-entrant Coaxial Optical Path and Experimental Verification *

Jin-Bao Yang(杨金宝)[1,2,4**], Jian-Guo Liu(刘建国)[1,2], Ning-Hua Zhu(祝宁华)[1,3], Li-Juan Yu(于丽娟)[1]

[1]*Laboratory of Solid State Optoelectronic Information Technology, Institute of Semiconductors, Chinese Academy of Sciences, Beijing 100083*

[2]*School of Electronic, Electrical and Communication Engineering, University of Chinese Academy of Sciences, Beijing 100049*

[3]*College of Materials Science and Opto-Electronic Technology, University of Chinese Academy of Sciences, Beijing 100049*

[4]*Science and Technology on Optical Radiation Laboratory, Beijing Institute of Environmental Features, Beijing 100854*

(Received 12 June 2017)

To overcome the shortcomings of the traditional passive ranging technology based on image, such as poor ranging accuracy, low reliability and complex system, a new visual passive ranging method based on re-entrant coaxial optical path is presented. The target image is obtained using double cameras with coaxial optical path. Since there is imaging optical path difference between the cameras, the images are different. In comparison of the image differences, the target range could be reversed. The principle of the ranging method and the ranging model are described. The relationship among parameters in the ranging process is analyzed quantitatively. Meanwhile, the system composition and technical realization scheme are also presented. Also, the principle of the method is verified by the equivalent experiment. The experimental results show that the design scheme is correct and feasible with good robustness. Generally, the ranging error is less than 10% with good convergence. The optical path is designed in a re-entrant mode to reduce the volume and weight of the system. Through the coaxial design, the visual passive range of the targets with any posture can be obtained in real time. The system can be widely used in electro-optical countermeasure and concealed photoelectric detection.

PACS: 42.30.Tz, 42.30.Va DOI: 10.1088/0256-307X/34/12/124202

Photoelectric ranging technology was mainly divided into active ranging technology and passive ranging technology. Active ranging technology was mainly in the mode of laser ranging. By emitting a continuous or pulsed laser to irradiate the target and receiving object echo signal, the target's range information was retrieved according to the time or phase information.[1−4] The largest disadvantage of active mode was poor concealment.[5] Although 1.54 μm, 10.4 μm or other eye invisible spectral band lasers were used to improve the concealment,[6,7] the lasers could still be detected by a proper photo detector. Therefore, it is difficult to meet the increasing complex requirements in photoelectric countermeasure application field.

Visual passive ranging technology has been the focus of research institutions over the world, which can meet the urgent needs of optoelectronic countermeasures in the future.[8,9] In visual passive ranging technology, the range of objects was determined by detecting the natural light radiated by objects. At present, the most typical visual passive ranging methods are the binocular triangulation ranging technology,[10,11] ranging technology based on lens imaging formula,[12] and ranging technology based on the target radiation and transmission characteristics.[13] In recent years, the photoelectric passive ranging technology is developing towards miniaturization, low power consumption and high reliability. Passive ranging technology based on image information will be an important direction in the future.[14] In this study, a new method based on re-entrant coaxial optical path is presented, which is different from traditional passive ranging technologies. In this method, the imaging difference of arbitrary attitude target is obtained by designing the re-entrant optical structure at the imaging end, and then the target range was retrieved. It could solve the problems of large range error in long distance, complex calibration, difficult to reduce the volume and weight of the traditional electro-optical passive ranging method. In all, the design has the advantages of high precision, small size, light weight and good stability.

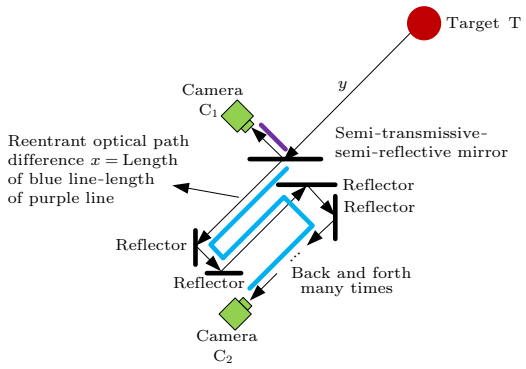

Fig. 1. Schematic diagram of the re-entrant coaxial optical path.

The ranging principle of the visual passive ranging method is shown in Fig. 1. Through the re-entrant

*Supported by the National Basic Research Program of China under Grant No 2014CB340102.

**Corresponding author. Email: yangjinbao20054723@126.com

coaxial design, the visual passive ranging of the targets with any posture could be achieved in real time. In Fig. 1, C_1 and C_2 are imaging cameras with the same performance and parameters, and T is the target with any posture in air. The distance between T and C_1 is y. The optical path difference (OPD) is x, which is formed by turning back and forth through optical path many times after the target echo signal into camera C_1. The camera resolution is set to be $a \times b$ and the instantaneous field of view of the two cameras is θ (with horizontal field of view as an example, radian sign). At the imaging moment, the optical cross-sectional area of target is A. The enclosed imaging area on focus plane array (FPA) of the C_1 camera is S_1, and the enclosed imaging area on FPA of the C_2 camera is S_2. According to the principle of imaging geometry, we have the formulas

$$\frac{A}{\frac{a}{b}(2y\tan\frac{\theta}{2})^2} = \frac{S_1}{ab}, \tag{1}$$

$$\frac{A}{\frac{a}{b}[2(y+x)\tan\frac{\theta}{2}]^2} = \frac{S_2}{ab}. \tag{2}$$

Because the camera C_1 is closer to the target than C_2, we can obtain $S_1 > S_2$. Using Eqs. (1) and (2), we obtain

$$y = \frac{x}{\sqrt{\frac{S_1}{S_2}} - 1}. \tag{3}$$

On the one hand, different from the traditional passive ranging method which is based on external baseline imaging,[15] the present method could passively locate arbitrary target objects without the support of a large number of feature databases. On the other hand, the key idea of binocular triangulation ranging technology is that it obtains the target range through matching images. Binocular triangulation ranging method is suitable for short range. As the range increases, because of the step response of imaging device, range jump may exist in pixels of long range (more than 1 km) target, causing great ranging error for remote targets. In addition, high precision image matching increases the algorithm complexity and computational complexity, thus the present method is difficult to use in the engineering field with high real-time requirement. In a word, compared with the traditional passive ranging technology, the visual passive ranging method in this study has the advantages of simple system, high reliability, reliable distance measurement, easier engineering and stronger practicability.

Setting the image area difference of two cameras to be d ($d = S_1 - S_2$), Eq. (3) could be written as

$$\frac{S_2 + d}{S_2} = \left(1 + \frac{x}{y}\right)^2. \tag{4}$$

When Eq. (4) is derivative, the expression of ranging error could be obtained as follows:

$$\Delta y = \frac{y^3}{2x(x+y)S_2}\Delta d, \tag{5}$$

where Δy is the ranging error, and Δd is the pixel error of the two camera image difference. To achieve higher ranging accuracy (smaller ranging error), the OPD between the two cameras and the number of target pixels on the imaging plane should be increased. At the same time, the ranged object should be as close as possible to the passive ranging system. In addition, a direct relationship exists between Δy and Δd. At present, the image difference between the two cameras could be one pixel, namely, $\Delta d = 1$. Figure 2 shows the relationship between the ranging error Δy and range y.

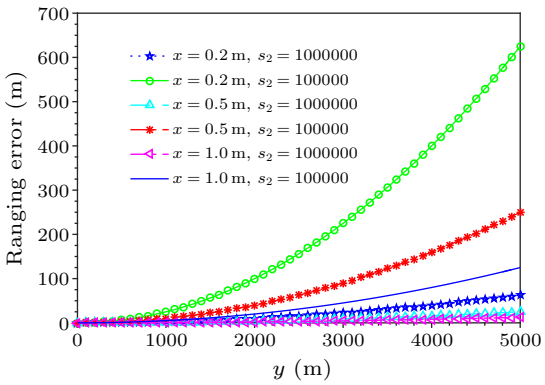

Fig. 2. Relationship between the ranging error Δy and range y.

From Fig. 2, the ranging error increases as the range increases. Because of the limitation of OPD, by increasing the area of the target image, the ranging error could be maintained at a low level. Take the target horizontal direction as an example, and suppose the target imaging feature size to be t. The range between camera C_1 and target is y, and the distance between camera C_1 and camera C_2 is x. The horizontal field of view of both the cameras is θ (radian sign). The resolution of the camera in the target feature size dimension is M. The imaging relationship is shown in Fig. 3.

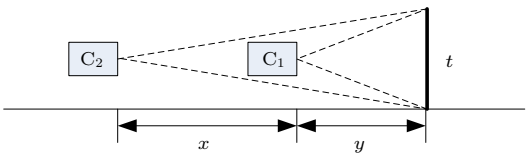

Fig. 3. Imaging geometric diagram.

Because of the existence of OPD x, the viewing angles of the two cameras to the same target are different. To distinguish the difference between the view angles of the target generated by the two cameras, the difference should be no less than the instantaneous field of view of a single pixel of the camera. Because $y \geq 10t$ generally, we have

$$\tan\frac{t}{y} \approx \frac{t}{y}. \tag{6}$$

The above theoretical relationships could be expressed

as

$$\frac{t}{y} - \frac{t}{x+y} \geqslant \frac{\theta}{M}, \tag{7}$$

$$y \leqslant \frac{\sqrt{x^2 + (4xtM/\theta)} - x}{2}. \tag{8}$$

Formula (8) shows the function relationship among the range y, the feature size t of the target, OPD x and the resolution M of the camera in the target feature size dimension. The maximum ranging is

$$y_{\max} = \frac{\sqrt{x^2 + (4xtM/\theta)} - x}{2}. \tag{9}$$

For a better analysis of the relationship among the parameters, setting $u = y_{\max}$, then we obtain

$$u = \frac{\sqrt{x^2 + (4xtM/\theta)} - x}{2}. \tag{10}$$

Since $u = u(y, M, t, \theta)$ is functions of x, M, t and θ. The full division of u is

$$\begin{aligned} d_u = {} & \frac{1}{2}\left[\frac{x + (2tM/\theta)}{\sqrt{x^2 + (4xtM/\theta)}} - 1\right]\frac{\partial u}{\partial x} \\ & - \frac{1}{2}\left[\frac{2xtM}{\theta\sqrt{x^2\theta^2 + 4xtM}}\right]\frac{\partial u}{\partial \theta} \\ & + \frac{1}{2}\left[\frac{2xt}{\sqrt{x^2\theta^2 + 4xtM}}\right]\frac{\partial u}{\partial M} \\ & + \frac{1}{2}\left[\frac{2xM}{\sqrt{x^2\theta^2 + 4xtM}}\right]\frac{\partial u}{\partial t}, \end{aligned} \tag{11}$$

$$\frac{x + \frac{2tM}{\theta}}{\sqrt{x^2 + (4xtM/\theta)}} - 1 > 0, \tag{12}$$

$$-\frac{2xtM}{\theta\sqrt{x^2\theta^2 + 4xtM}} < 0, \tag{13}$$

$$\frac{2xt}{\sqrt{x^2\theta^2 + 4xtM}} > 0, \tag{14}$$

$$\frac{2xM}{\sqrt{x^2\theta^2 + 4xtM}} > 0. \tag{15}$$

From Eqs. (11)–(15), u is positively correlated with the OPD x, the camera resolution M and the target feature size t, while u is negatively correlated with the imaging field angle θ. Therefore, to increase the value of $y_{\max}$, the OPD x should be increased, the imaging field angle θ should be decreased, and the resolution of imaging detector should also be increased. Meanwhile, the feature size of the target should be as large as possible. In practical applications, the imaging resolution M and the field of view angle θ of the camera are fixed values, which are M_0 and θ_0, respectively. Assuming that the feature size of target which could be ranged by the system is t_0, when the practical target feature size $t > t_0$, the system could realize effective ranging.

When the feature size is t_0, the relationship of the maximum effective range u and the OPD x can be expressed as

$$u = \frac{\sqrt{x^2 + (4xt_0M_0/\theta_0)} - x}{2}. \tag{16}$$

HK VISION's high resolution camera DS-2CD40C5F could be used, with a resolution of $4k \times 3k$ and a target size of 1/1.7 inch. The lens is taken as HD60 from Fuji corporation, with a maximum focal length 1700 mm. Setting $\theta_0 = 0.01$ rad and $M_0 = 4000$, the function of the maximum ranging distance and the OPD x could be expressed as

$$u = \frac{\sqrt{x^2 + 1600000t_0x} - x}{2}. \tag{17}$$

When t_0 takes different values, the function curve of the maximum ranging u and the OPD x is shown in Fig. 4.

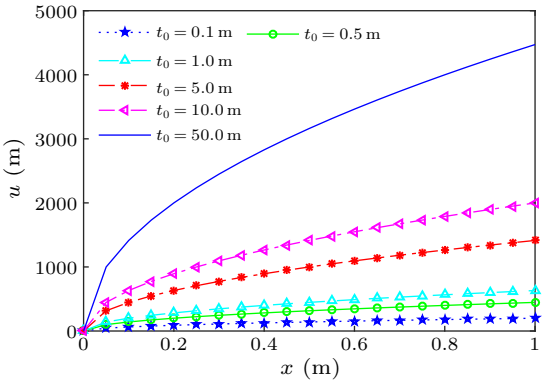

Fig. 4. Relationship diagram of u and x, with $\theta_0 = 0.01$ rad and $M_0 = 4000$.

It could be seen from Fig. 4 that with the increase of the OPD and the target feature size, the maximum range also increases. Considering that the OPD is limited by the volume and weight of the system and the imaging angle, in the actual application, the resolution of the image or the feature size of the target is increased, which is easy to implement in engineering.

Based on the design of re-entrant coaxial optical path, the system device is shown in Fig. 5. The system includes a unit of optical transparent and reflective mirrors, an imaging unit, and a visual range inversion unit.

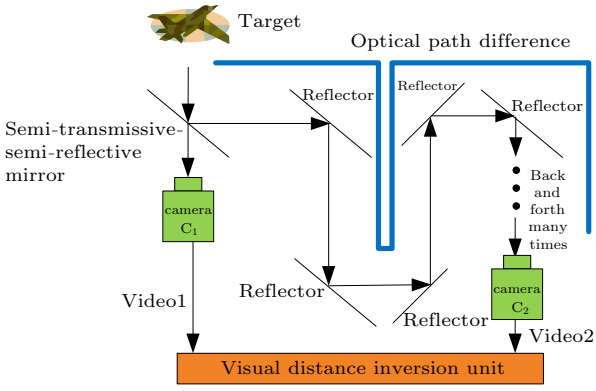

Fig. 5. Composition diagram of the passive ranging system.

The unit of optical transparent and reflective mirrors, which is composed of a semi-transmissive-semi-reflective mirror and multiple reflectors, completes the

optical path splitting and reflection of the target reflected echo signal. After passing through the semi-transmissive-semi-reflective mirror, the target echo signal is split into two parts. One part of the signal is transmitted through the C_1 camera into the imaging unit, and the other is reflected into the subsequent mirror group. This part of the signal light makes optical path extension within the mirror group, forming a certain OPD over the transmitted portion of the signal light. Finally, it enters the imaging unit of the C_2 camera for imaging. The size of the OPD is determined by the number of mirror groups and the distance of adjacent mirrors.

The imaging unit includes cameras C_1 and C_2. In this scheme, cameras C_1 and C_2 have the same imaging resolution and the same optical modulation lens, so as to ensure that the target echo signal enters the imaging device with the same performance after the optical path split. The external noise interference is also reduced accordingly.

The visual distance inversion unit receives the image signals of cameras C_1 and C_2. Since the optical transmission time caused by OPD is very short, which even could be ignored, we can consider that the target image is obtained by cameras C_1 and C_2 at the same time. In other words, the unit shows real-time passive ranging performance. Visual range inversion unit completes the edge extraction of target image through the image processing algorithm firstly, and then calculates the target image area, and finally makes inversion of the target range according to Eq. (3).

Due to the difference in optical path between the imaging cameras C_1 and C_2, the imaging sizes of the target on both cameras are different. The higher the resolution is, the larger the imaging size difference is. Thus the inversion of target range would show higher accuracy. In addition, through the re-entry structure design, the system is simplified apparently and the size and weight of the system are also reduced obviously. The real-time performance of the design makes the system achieve real-time visual passive ranging to target with arbitrary posture.

The principle of this method is verified by experiment. To facilitate the precise control of OPD, the experimental scheme uses the equivalent method with target movement and camera fixation. To ensure the adequacy, the experiment is divided into two groups. When the value of OPD is small, the magnitude is in centimeters. When the OPD is large, the magnitude is in meters.

In the centimeter experiment, a black and white board with a black rectangular pattern is used as a target. The length of the black rectangle is 0.12 m, while the width is 0.07 m. Take the black rectangle horizontally as the direction of the characteristic dimension. Camera resolution is 1280×720, and $M = 1280$. The horizontal viewing angle of the camera $\theta = 0.09$ rad is calibrated. The initial range between the camera and the target is $y_0 = 1.00$ m.

Here the OPD x is set to be 0 cm, 1 cm, 2 cm, 3 cm and 4 cm. Several sets of experimental data and the calculated data according to Eq. (3) are listed in Table 1.

Table 1. Ranging parameters in the centimeter experiment.

OPD x (cm)	Target area	Measured value y (m)	Error (m)	Error ratio	Note appended
0	46189	1.00 (y_0)	0	0	Calibrated data
1	45120	0.85	−0.15	15%	Tested data
2	44240	0.92	−0.08	8%	Tested data
3	43646	1.04	0.04	4%	Tested data
4	42780	1.02	0.02	2%	Tested data

Table 2. Ranging parameters in the meter experiment.

OPD x (cm)	Target area	Measured value y (m)	Error Δy (m)	Error ratio	Note appended
0	89282	38.52 (y_0)	0	0	Calibrated data
1.07	84230	41.90	3.38	8.76%	Tested data
2.14	80087	40.71	2.19	5.67%	Tested data
3.21	76037	39.61	1.09	2.84%	Tested data

Table 3. Ranging parameters in different ranges.

Target area S_2	Target area S_1	Ranging value y (m)	Actual value $y*$ (m)	Error Δy (m)	Error ratio $\Delta y/y*$
84770	90195	33.97	37.48	3.51	9.36%
106150	112600	35.75	33.20	2.55	7.68%
128803	138788	28.13	29.99	1.86	6.20%
157605	170970	25.76	26.78	1.02	3.81%
170970	185887	25.05	25.71	0.66	2.57%
241484	265862	21.72	21.43	0.29	1.35%
293020	326500	19.25	19.29	0.04	0.21%

In the meter experiment, a black board with an A3 paper (420 mm×297 mm) is used as a target. Take the horizontal direction of the black rectangle target as the characteristic dimension for example. The camera resolution is 1920×1080, and $M = 1920$. The horizontal viewing angle of the camera θ is calibrated to be 0.037 rad in the lab. The initial range between the camera and the target is $y_0 = 38.52$ m.

Taking the length of floor brick as a measurement scale, the minimum moving distance of target is the

length of floor brick, which is 1.07 m. The OPD is 1.07 m, followed by 2.14 m, 3.21 m, according to the number increase of floor bricks.

Several sets of experimental data and the calculated data according to Eq. (3) are listed in Table 2.

To analyze the relationship between range error and range under the same OPD and different ranges, the OPD $x = 1.07$ m is set up, and the ranging data at different ranges is listed in Table 3. From Table 3, it could be seen that the ranging error increases with the range, which proves the correctness of the theoretical analysis of Eq. (5).

From the above experiments, the visual passive ranging method based on re-entrant coaxial optical path is reasonable and feasible with ranging error less than 10%. In the process of ranging, no calibration is needed. Moreover, the error convergence is good, and it is easy to implement in engineering. The actual ranging error is greater than the theoretical error, mainly because there is pixel loss in the imaging and target edge extraction, which leads to measurement errors.

In summary, a new visual passive ranging method based on re-entrant coaxial optical path has been presented. The principle of the method is described in detail, and the relationships among the parameters are analyzed quantitatively. The system composition scheme is proposed and the simplified equivalent experiment is adopted to prove the principle of the system. The experimental results show that the method is correct, and the principle is feasible. The method overcomes the shortcomings of the traditional image-based passive ranging scheme, such as large ranging error for remote target and difficult to converge. It has the advantages of small ranging error (generally less than 10%) and good robustness. The actual test ranging error of this method is lower than that of the traditional photoelectric passive ranging method.[16,17] In practice, to achieve higher ranging accuracy, the OPD and image resolution can be increased. Also, the target extraction algorithm can be optimized to reduce the pixel loss. The use of re-entry coaxial optical path design reduces the volume and weight of the system. Above all, the system is easy to realize the miniaturization design, and can be used for real-time visual passive ranging of objects with arbitrary posture.

References

[1] Amann M C, Bosch T M, Lescure M, Myllylae R A and Rious M 2001 *Opt. Eng.* **40** 10
[2] Yang X, Zhao Y, Xu L, Yang C H, Wang Q, Liu Y H and Zhao Y 2015 *Chin. Phys.* B **24** 104203
[3] Gomaa W, Elsherif A F and Elsharkawy Y H 2015 *Proc. SPIE* **9342** 934221
[4] Li Y Q, Luo Z R, Liu H S, Dong Y H and Jin G 2012 *Chin. Phys. Lett.* **29** 079501
[5] Steinvall O, Persson R, Berglund F, Gustafsson O and Gustafsson F 2014 *Proc. SPIE* **9080** 90800W-1
[6] Poujouly S, Joumet B and Placko D 1999 *Proc. IEEE Conf. Ind. Electron. Soc.* **3** 1312
[7] Foy B R, McVey B D, Petrin R R, Tiee J J and Wilson C W 1995 *Proc. SPIE* **4370** 181
[8] Jarvis R A 1983 *IEEE Trans. Pattern Anal Machine Intell.* **PAMI-5** 122
[9] Dowski E R and Cathey W T 1994 *Appl. Opt.* **33** 6762
[10] Lopez J, Markel M, Siddiqi N and Gebert G 2003 *ICIP 2003 Proceedings* **1** 929
[11] Du Y L and Lu J 2014 *Conf. Communication Control (IMCCC)* **196** 932
[12] Fug J, Huang S H and Zhang G P 1995 *Proc. SPIE* **2599** 64
[13] Anderson J R, Hawks M R and Gross K C 2011 *Proc. SPIE* **8020** 802005
[14] Fu X N, Liu S Q and Lie K 2007 *Proc. SPIE* **6279** 62793A-1
[15] Baldacci A, Corsini G and Diani D 1999 *Proc. SPIE* **3720** 473
[16] Huang S K, Xia T and Zhang T X 2007 *Infrared Laser Eng.* **36** 109 (in Chinese)
[17] Xu Z H and Zheng M 2005 *Ship Electron. Eng.* **25** 127 (in Chinese)